Global analysis of floating offshore wind turbines with shared mooring system

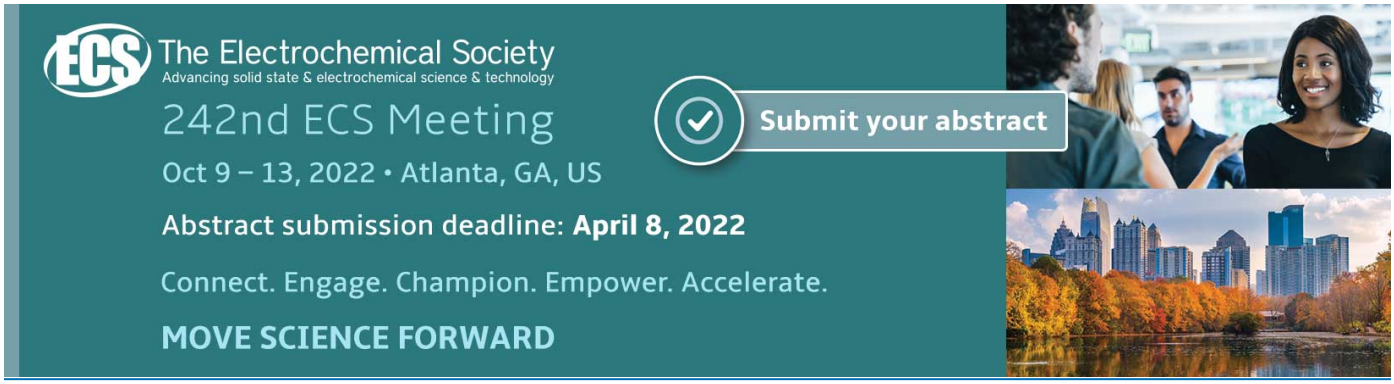

Global analysis of floating offshore wind turbines with shared mooring system

H Munir, C F Lee* and M C Ong

Faculty of Science and Technology, University of Stavanger, Norway

* Contact author: chern.f.lee@uis.no

Abstract. Floating wind turbines (FWTs) with shared mooring systems can be one of the most cost-effective solutions in reducing mooring costs. First, the static configuration of a shared line is estimated using the elastic catenary equation. The present study investigates the global responses of two FWT with a shared mooring system. Two shared mooring configurations with different horizontal distances between the FWTs are considered. In the first configuration, the FWTs are placed 750m apart; and in the second configuration, they are placed 1000m apart. Two different environmental conditions (ECs) are used to simulate the global responses of the system in time domain. The shared mooring line results in higher extreme motions in surge and sway (degree of freedoms) DOFs due to the reduction of mooring restoring stiffness. The lower mooring restoring stiffness can be attributed to the reduction of one seabed anchoring point for each FWT as compared to a single FWT with three anchors installed. In the rotational DOFs, the shared mooring line configurations result in slight mean offset in each direction and significant increase in the motion standard deviations. This is caused by the reduced mooring stiffness associated with the change in platform orientation.

1. Introduction

Floating Wind Turbines (FWTs) is getting more attention in the wind energy sector during the last decade due to the availability of large wind resources at deeper waters. Better sea transport facilities like large towing vessels and heavy lift cranes have made this concept even more feasible. FWTs are becoming one of the most promising means of energy production, especially in deep-water regions. The reason behind this is the reduced friction offshore, the stronger wind production with small turbulence on average and to avoid noise and visualization pollution due to the large distance from populated areas [1]. Thus, a lot of research has been conducted around the design of FWTs to make it more efficient, cost effective and sustainable.

However, due to a requirement of a more compliant supporting structure to control the dynamic motions of the wind turbine within acceptable limits, the cost of the floating structure remains one of the biggest challenges in way of the full deployment of commercialized floating wind farms. The 5-MW-CSC is a braceless semi-submersible platform proposed in [1] to support the NREL 5-MW horizontal axes wind turbine [2]. Research on this concept is relatively less as compared to the other similar concepts like DeepCwind OC4 by [3], OC3-Hywind by [4] and WindFloat by [5].

One of the most promising way to minimize the levelized cost of energy (LCoE) is to reduce the structural weight by minimizing the number of components. When considering the floating offshore wind farms (FOWFs), sharing of mooring lines between neighboring FOWTs is an attractive concept to reduce the LCoE and the complexity of installation activities. The total number of mooring lines is decreased through the sharing of mooring line between two adjacent floating wind turbines (FWTs). The number of anchors required lowers as well, resulting in further cost reduction.

In the present study, the global responses of two 5-MW-CSC FWTs with one shared mooring line in extreme wind and wave conditions are investigated. To provide comparability with the results presented by Luan et al. [1], the specifications of the mooring lines that run from the fairleads to anchors remain unchanged. For the shared mooring line, the static configuration is estimated using elastic catenary equation.

The motion responses are calculated using time domain simulations and compared against the case of a single FWT presented by Luan et al. [1].

2. CSC wind turbine & methodology

2.1. CSC floating wind turbine

The supporting platform of a 5-MW- CSC was designed to accommodate a 5-MW NREL offshore base line wind turbine. The 5-MW-CSC is composed of a rotor nacelle assembly (RNA), tower, hull and mooring system as shown in Figure 1. The hull of 5-MW-CSC consists of one central, three side columns and three pontoons. The tower is mounted on the central column in the middle from which the three side columns are placed at an equidistant offset. The ballast mass is symmetrically distributed about the central line of the central column. Ballast water is used to achieve the operating draft and the pontoons are completely filled with ballast water. The hull structure is modelled as a rigid body with master-slave connections to the tower base and the fairleads for mooring line connections. The mooring system is composed of three catenary chain mooring lines spread symmetrically at 120^0 about the z_g-axis of the platform. The chain mooring lines are simplified as a uniformly distributed mass with a solid cross-section as proposed in [1]. The body fixed coordinate system of 5-MW-CSC is coincident to the global coordinate system. The 0^0 and 90^0 directions are defined as the positive directions in x_g and y_g, respectively as shown in Figure 2. In the present study, hydrodynamic studies for the 5-MW-CSC hull have been performed using the linear potential flow program WADAM [6] and validated against the result presented by Luan et al. [1]. The hydrodynamic coupling (added mass and damping) between the two FWTs is neglected due to the long distance between the two rigid bodies. The response amplitude operators (RAOs) in different wave directions for the surge, heave and pitch DOFs are presented in Appendix A.

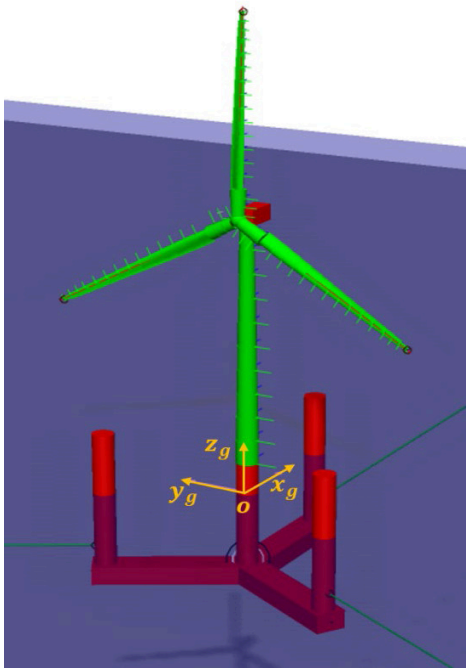

Figure 1: CSC-5-MW single wind turbine model.

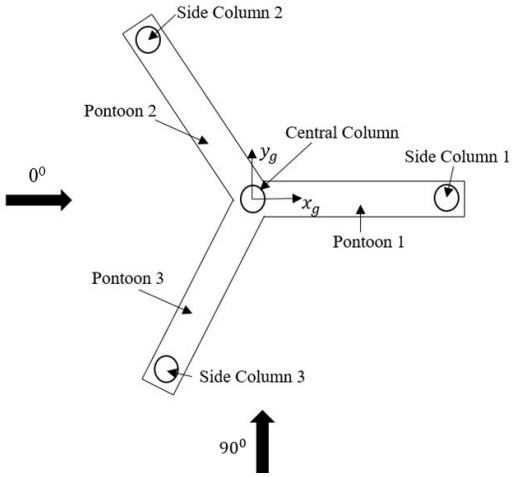

Figure 2: Top view of the hull of 5-MW-CSC.

2.2. Single mooring lines modelling

Mooring lines are station keeping devices which are designed in such a way to provide a sufficient restoring force for the floating platforms in various environmental conditions. The 5MW-CSC FWT is moored with three catenary chain mooring lines spread symmetrically at 120° about the platform z-axis as described in [1]. Same configurations are used in the present study for single mooring lines design in which each wind turbine is modelled with two side catenary chain single mooring lines spread at 120° and one shared mooring line. The stiffnesses of mooring lines consist of material and geometrical stiffness. The force-displacement properties of a catenary system are dependent on material properties, line geometry and mooring system configuration. The single mooring line properties are summarized in Table 1. Moreover, the static configuration and effective tension of the used catenary single mooring lines are presented in Figure 3 and Figure 4, respectively.

Table 1. Single mooring line properties.

Property	Value
Mooring line type [-]	Chain
Mooring line mass density [kg/m]	115
Un-stretched mooring line length [m]	1,073
Mooring line diameter [m]	0.137
Extensional stiffness of mooring line [kN/m]	3.08 x 10^6
Depth of fair lead below sea water line (SWL) [m]	18
Depth of anchors [m]	200
Density of material [kg/m^3]	7,850

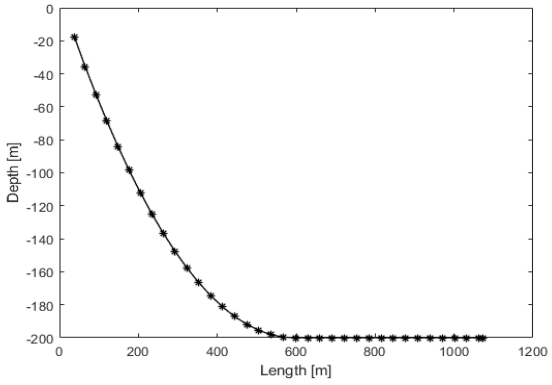

Figure 3. Single mooring line shape in dual CSC system.

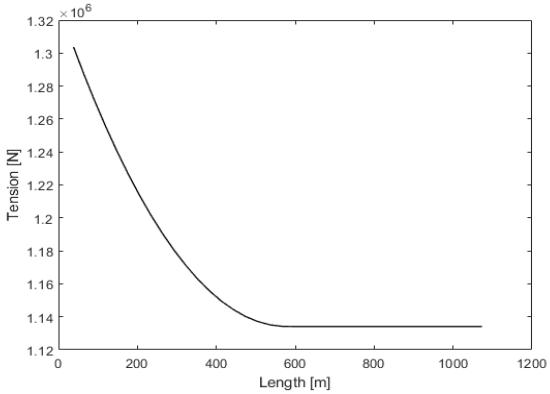

Figure 4. Axial effective tension of single mooring line.

2.3. Shared mooring line modelling

Basic catenary equations are applicable for shared mooring line design when the two fairleads are on the same level. The mooring line can be designed as two symmetric lines shape connected at the sagging point. Various assumptions are made against the modelling of a shared mooring line such that the dynamic effects, bending effects and current forces effects on mooring lines can be neglected as proposed by Liang et al. [7]. The origin of the catenary plane is set at the fairlead as shown in Figure 5. By setting one end of the shared line as the origin of a catenary plane, the elastic catenary equations, Eqn. 1 and Eqn. 2 are applied [7].

$$x = \frac{H}{w}\log\left(\frac{\sqrt{H^2+V^2}+V}{H}\right) + \frac{H}{EA}s \quad (1)$$

$$h = \frac{1}{2}\frac{ws^2}{EA} + \frac{H}{w}\left[\frac{1}{\cos\emptyset} - 1\right] \quad (2)$$

where x and h are the horizontal and vertical distance of the sagging point measured from the fairlead, H and V are the horizontal and vertical components of the mooring tension T at the fairlead 1, s is the total suspended length of the shared line, w is the weight per unit length of the mooring line in water, EA is the extensional stiffness of the line with E as the elastic modulus and A is the cross-sectional area. With the distances between the fairlead and the sagging point known and with an initial guess of s and h, the final suspended length can be solved by iteration. The resulting tension at fairleads can then be calculated. The tension of the shared mooring line is adjusted to achieve horizontal force balance by modifying the vertical distance of the sagging point.

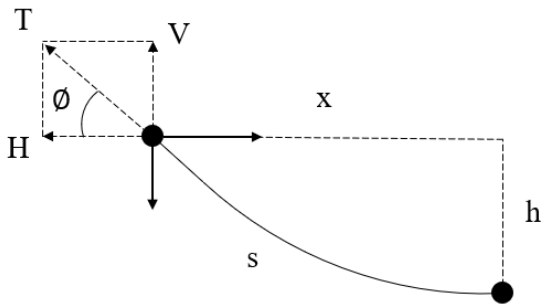

Figure 5. Illustration of shared line in catenary plane.

The properties of shared mooring line and its static configurations are shown in Table 2 and in Figure 6, Figure 7 & Figure 8.

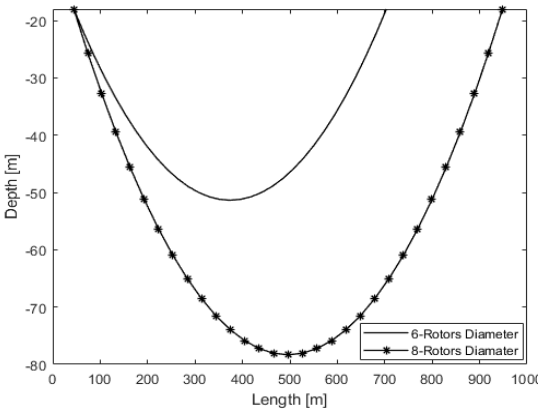

Figure 6. Line shape in the catenary plane for the shared line.

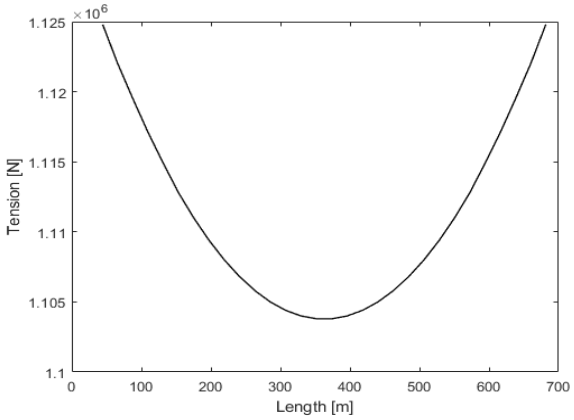

Figure 7. Shared line tension with 6 rotors diameter configuration.

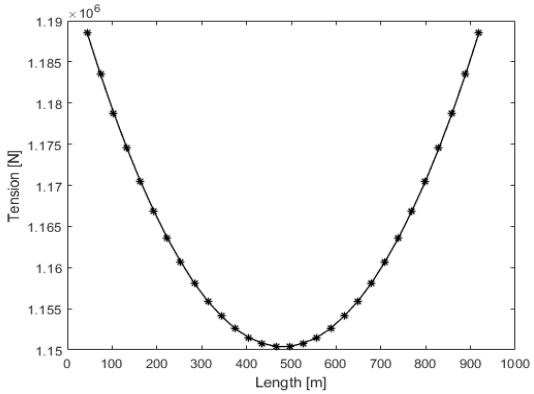

Figure 8. Shared line tension with 8 rotors diameter configuration.

Wind turbines configuration

In the present study, two different shared line configuration are investigated. In the first configuration, the FWTs are placed 750m (six rotor diameters) apart; in the second configuration, they are placed 1000m (8 rotor diameters) apart. In order to accommodate the shared mooring line, the floating platforms are rotated by 30^0 and -30^0 for FWT 1 and FWT2, respectively as compared to the original 5MW-CSC FWT. A plan view of the two-FWT configuration is as shown in Figure 9. Following the recommendation by Liang et al. [7], the properties of the shared mooring line are summarized in Table 2. Two wind turbines are placed with shafts along the x_g-axis in the global coordinate system with the wind turbines facing the upwind direction as shown in Figure 9. The focus in the present study is the comparison of responses of FWTs with waves coming from 0^0 to 180^0 against the responses of a single FWT. Wind is constantly directed at 0^0 (positive x_g-direction) into the rotor plane of wind turbines. The shared line is positioned along the sway direction (y_g) in the present model. The shared line is modelled using 30 bar elements with a total length of 661.4 m and 911.4 m for the first and second configuration, respectively.

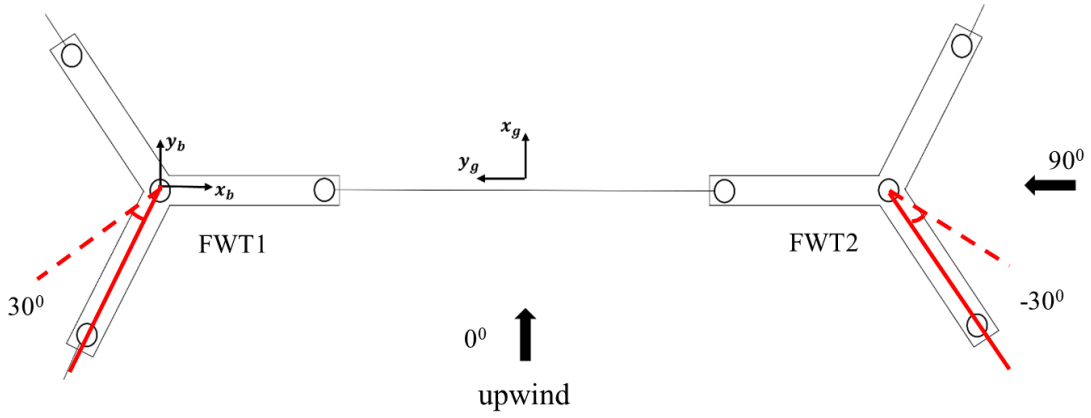

Figure 9. Floating Wind Turbines Configuration.

Table 2. Shared Mooring Line Properties for CSC-Wind Turbines at Two Horizontal Distances.

Property	Value
Mooring line type [-]	Chain
Mass density [kg/m]	72
Diameter [m]	0.06
Weight in water [N/m]	649.46
Extensional stiffness [N]	3.38×10^8
Maximum breaking load [N]	4.52×10^6

3. Environmental conditions (ECs)

Joint probability density function (PDF) of mean wind speed (U_W), significant wave height (H_S) and peak period of wave spectrum (T_P) and the environmental contour of U_W, H_S and T_P corresponding to a 50-year return period are described in [8]. Two parameter JONSWAP spectrum is employed with a peak factor of 3.3 to describe the waves while the wind is described by the Kaimal wind spectrum with normal turbulence. Turbulent wind fields are generated using Turbsim [9] and as a simplification, it is assumed that both wind turbines are experiencing identical wind field in each EC. In order to assess the global responses of FWTs, one operational loading condition above the rated wind speed for wind-dominant case and one extreme loading condition for wave-dominant case with parked wind turbine are considered [10, 11] as listed in Table 3. For each EC, H_S is selected as the maximum value on the contour surface corresponding to the chosen U_W. Seven different wave incident directions varying from $0°$ to $180°$ with $30°$ interval is used to consider the effects of waves coming from different directions.

Table 3. Environmental Conditions for global response study.

	Turbulence Intensity [%]	Wind Speed [m/s]	Hs [m]	Tp [s]	Note
EC1	12	20	10.3	14.7	Operational
EC2	11	40.4	15.3	14.3	Parked

4. Results and discussions

4.1. Case study A

To obtain the global responses of the FWTs under wind and wave loads, numerical simulations are carried out in time domain using SIMA, a simulation software for marine operations [12, 13]. To account for statistical uncertainty, six 1-hr simulations with distinct random seeds are carried out. The average statistical properties based on six 1-hr simulations are plotted in Figure 10. In the present paper, the platform motions of both FWTs connected with a shared mooring line are to be compared against the platform motions of a single FWT. As such, for each platform's DOF, one most significant wave direction is selected, and the corresponding average statistical properties are summarized in Table 4. In comparison, the statistical properties for a single FWT under the same environmental loads and incident wave directions documented in [1] are presented in Table 5.

For EC1, with a 0^0 incident wave direction, the mean surge offsets of FWT1 and FWT2 are similar to the case of a single FWT. However, both FWT1 and FWT2 achieve higher maximum and lower minimum surge motion, suggesting a lower mooring restoring stiffness in the surge direction. The lower mooring restoring stiffness can be attributed to the reduction of one seabed anchoring point for each FWT as compared to a single FWT with three anchors installed. Similar behavior in the surge direction can be observed under EC2, with an even greater difference in the negative surge direction.

For sway DOF, the response in 90^0 incident waves is compared. The mean positions of both FWT1 and FWT2 increase as compared to a single FWT and the increment is more significant in EC2 due to the higher waves. Both FWT1 and FWT2 achieve higher maximum and lower minimum sway motion due to the reduced mooring restoring stiffness in the sway direction. The shared mooring configuration increases the standard deviation of sway motion by approximately 50% and 22% for EC1 and EC2, respectively as compared to the single FWT. As expected, the heave motions of both FWT1 and FWT2 are dominated by buoyancy force and are in general displaying the same characteristic as compared to the case of a single FWT.

Based on the above observations, it is shown that the shared mooring line has a considerable effect on surge and sway motions of the platforms. The effect of a reduction in mooring restoring stiffness in the horizontal translational DOF is reflected through an increase in mean and maximum horizontal offset of the FWTs. The increase is more significant in the sway DOF as only two mooring lines are contributing to the restoring force of both FWTs.

For pitch DOF, the response in 0^0 incident waves is compared. The pitch motion of FWT1 is in general similar to the motion of a single FWT. However, FWT2 is having a smaller mean pitch angle in the downwind direction (-0.7^0). It is later observed that even when there is no wind, the neutral position of FWT2 is with a pitch offset of approximately 2^0 in the upwind direction. This has eventually resulted in FWT2 having a smaller mean pitch angle downwind. It is also shown that the use a shared mooring line resulted in an increase in the standard deviation of pitch motion. The increment is more prominent in EC1 with a 100% increment for FWT1.

For roll DOF, the response in 0^0 incident waves is compared. Roll motion is dominated by the influence of the shared mooring line. The configuration of the shared mooring line causes a mean roll offset that is different from the case with a single FWT. For FWT2, the shared mooring line configuration resulted in an increase in roll motion standard deviation by approximately 100% in EC1.

For yaw DOF, the responses of FWT1 and FWT2 in 120^0 incident waves is compared against the response of a single FWT in 90^0 incident waves due to different platform orientations. Significant reduction in the yaw standard deviation is observed for FWT2 in EC1.

Table 4: Maximum statistical properties of FWTs at 6 rotors diameter distance with different wave headings.

ECs	Turbines	Statistical Properties	Surge $*0^0$ [m]	Sway $*90^0$ [m]	Heave $*0^0$ [m]	Roll $*90^0$ [deg]	Pitch $*0^0$ [deg]	Yaw $*120^0$ [deg]
EC1	FWT1	Max	8.8	6.5	3	0.9	6.8	2.2
		Min	-0.9	-4.7	-3.4	-3.3	-0.2	-3.7
		Mean	3.6	0.8	-0.3	-1.2	3.3	-0.5
		Std	1.5	1.5	1	0.6	1	0.8
	FWT2	Max	9	6.4	3	7.2	1.6	2.4
		Min	-0.9	-4.9	-3.4	1.3	-3.1	-2.2
		Mean	3.8	-0.1	-0.3	4.3	-0.7	0
		Std	1.5	1.6	0.9	1	0.8	0.1
EC2	FWT1	Max	9.2	11.1	4.4	0.1	4	2
		Min	-5.1	-5	-4.7	-5	-2.5	-2.4
		Mean	1.6	-3.3	-0.2	-2.3	0.6	-0.1
		Std	2.1	2.2	1.3	0.7	0.8	0.6
	FWT2	Max	9.1	12.3	4.4	2.7	0.9	2.7
		Min	-5.1	-3.5	-4.7	-0.3	-3.6	-1.3
		Mean	1.5	2.9	-0.2	1.3	-1.1	0.5
		Std	2.1	2.3	1.3	0.4	0.5	0.6

* Incident wave direction

Table 5: Maximum statistical properties of single wind turbine proposed in [1].

ECs	Statistical Properties	Surge $*0^0$ [m]	Sway $*90^0$ [m]	Heave $*0^0$ [m]	Roll $*90^0$ [deg]	Pitch $*0^0$ [deg]	Yaw $*90^0$ [deg]
EC1	Max	8.5	4.5	3.5	3	6.8	1.9
	Min	-0.5	-4	-3	-2	0	-2.6
	Mean	3.5	0.1	0.1	0.5	3	-0.2
	Std	1.5	1	0.8	0.5	0.5	0.6
EC2	Max	10	9	5.5	3	4.2	1.8
	Min	-4.5	-5	-5	-4.2	-2.2	-2.1
	Mean	1.8	0.8	0.2	-0.3	0.5	0.1
	Std	2.1	1.8	1.5	0.6	0.5	0.5

* Incident wave direction

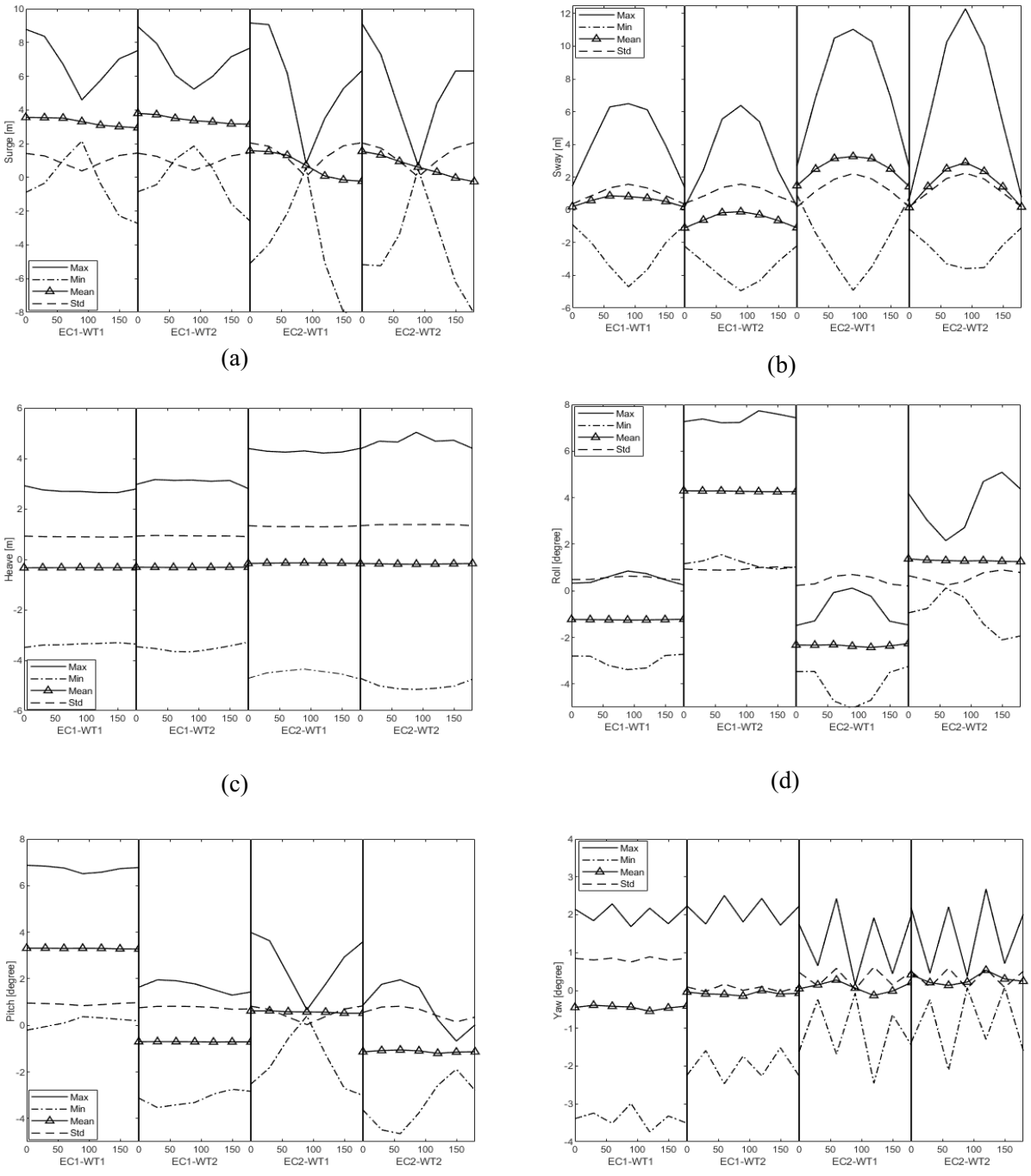

Figure 10: Statistical properties of dual 5-MW CSC at 6 rotors diameter distance in extreme combined wind and waves. For each condition, from the left end to the right end, wave direction varies from 0^0 to 180^0 with 30^0 intervals.

4.2. Case study B

In the second configuration, two wind turbines are placed at eight rotors diameter distance along the y_g-axis. A longer mooring line is used but with the rest of the properties remain the same as the first configuration. Similar procedure as described in Section 4.1 has been carried out to obtain the global responses of both FWTs. The average statistical results are plotted in Figure 11 and summarized in Table 6.

The second configuration aims at investigating the effect of varying distance between two FWTs. As discussed in Section 4.1, similar effect in the surge and sway DOF is observed. The mooring restoring stiffness in these two DOFs is reduced resulting in higher motion standard deviation as well as higher extreme motions. However, despite a slight change in sway mean offset, which is due to the design of the shared mooring line, motions in all DOF remain generally unchanged as compared to the first configuration. It demonstrates that changing the length of shared mooring line has little effect on the responses of FWTs. This is because the tension in a shared line contributes very little in restoring force and moment.

Table 6: Maximum statistical properties of FWTs at 8 rotors diameter distance with different wave headings.

ECs	Turbines	Statistical Properties	Surge $*0^0$ [m]	Sway $*90^0$ [m]	Heave $*0^0$ [m]	Roll $*90^0$ [deg]	Pitch $*0^0$ [deg]	Yaw $*120^0$ [deg]
EC1	FWT1	Max	8.7	5.7	3.1	1.3	6.8	2.3
		Min	-1	-4.8	-3.3	-3	-0.2	-3.7
		Mean	3.5	0.1	-0.2	-1	3.3	-0.5
		Std	1.4	1.5	0.9	0.6	1	0.8
	FWT2	Max	8.9	4.7	3.1	7.2	2	2.4
		Min	-0.9	-5.7	-3.3	1	-2.9	-1.5
		Mean	3.7	-0.6	-0.2	4.1	-0.4	0.4
		Std	1.5	1.5	1	1	0.8	0.5
EC2	FWT1	Max	9.2	10.5	4.5	0.2	4	1.9
		Min	-8	-4.1	-4.6	-4.5	-2.6	-2.3
		Mean	1.6	2.6	0	-2	0.6	-0.1
		Std	2.1	2.1	1.3	0.6	0.8	0.6
	FWT2	Max	9.1	9.6	4.5	2.5	1.2	2.8
		Min	-5.2	-4.6	-4.5	-0.4	-3.4	-1.3
		Mean	1.5	2.1	0	1.1	-0.8	0.5
		Std	2.1	2.1	1.4	0.4	0.6	0.6

* Incident wave direction

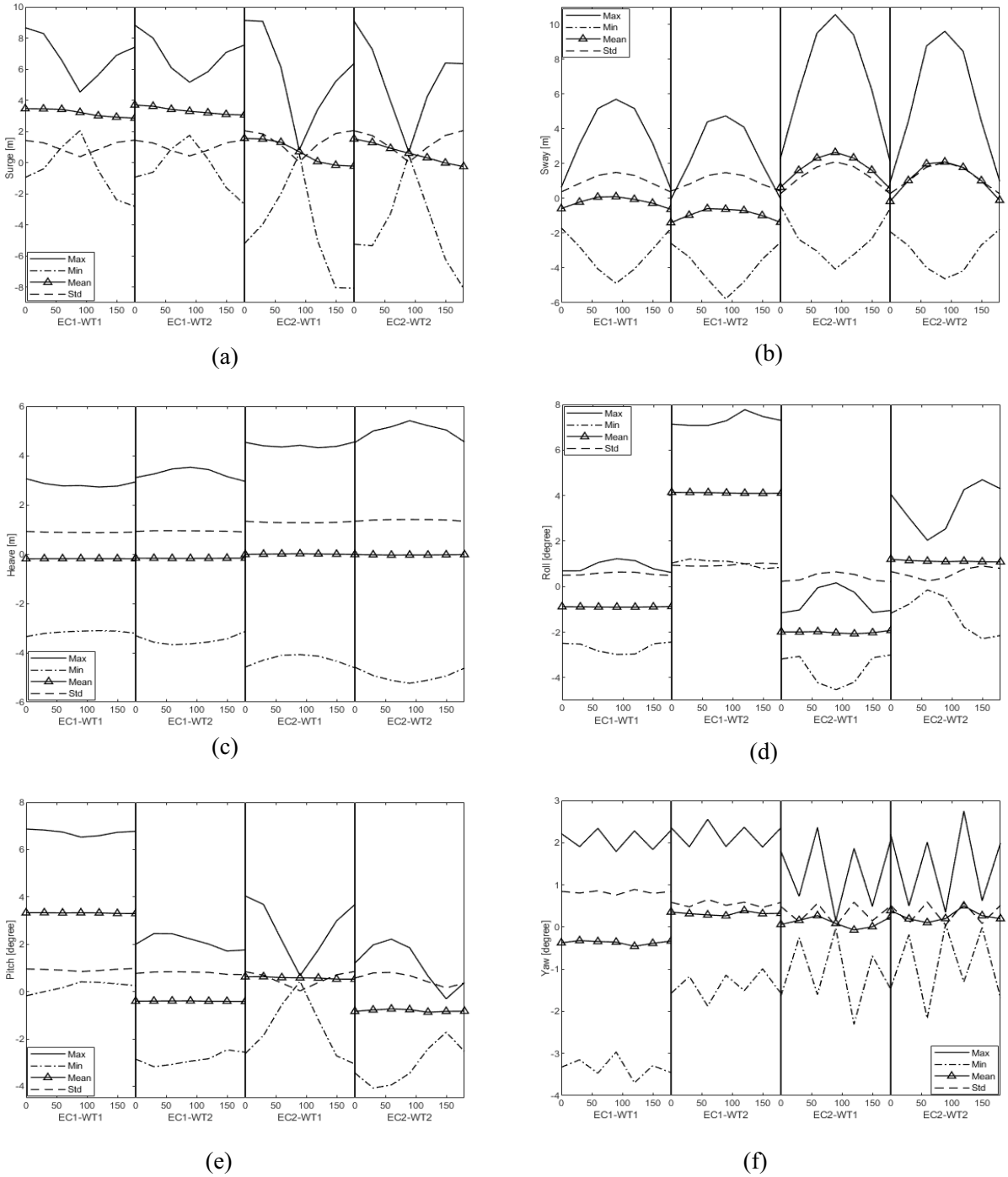

Figure 11: Statistical properties of dual 5-MW CSC at 8 rotors diameter distance in extreme combined wind and waves. For each condition, from the left end to the right end, wave direction varies from 0^0 to 180^0 with 30^0 intervals.

5. Conclusion and future works

The dual CSC-5MW FWTs with a shared mooring line at two horizontal distances are modelled in this paper. The rigid body motions in 6 DOFs of each wind turbines are compared against the single wind turbine model and discussed in Sections 4.1 and 4.2. Global time-domain analysis has been carried out to calculate the global responses in two selected combined wind and wave conditions. While a shared mooring system allows for cost saving s for floating wind farms, it also adds complexity to the dynamic behavior of the system. Basic catenary equation is employed to design the shared mooring line. The shared mooring line results in higher maximum motion and lower minimum motion in the surge and sway DOFs due to the reduction of mooring restoring stiffness. In the rotational DOFs, the shared mooring line configurations result in slight mean offset in each direction and significant increase in the motion standard deviations. This is caused by the reduced mooring stiffness associated with the change in platform orientation. The effect of different distances between FWTS has been investigated. For different distances between FWTs, the difference in motions in all DOF is not significant as the shared line contributes little to the restoring force.

The study in the present paper aims at establishing a model for preliminary investigation of dynamic behavior of two FWTs connected by a shared line. Future studies should be carried out focusing on the behavior in more specific environment conditions and detailed design of mooring line.

References

[1] Luan C, Gao Z and Moan T 2016 Design and analysis of a braceless steel 5-mw semi submersible wind turbine, *Int. Conf. on OMAE* (American Society of Mechanical Engineers) vol. 49972.
[2] Jonkman J, Butterfield S, Musial W and Scott G 2009 Definition of a 5-MW reference wind turbine for offshore system development (No. NREL/TP-500-38060). National Renewable Energy Lab.(NREL), Golden, CO (United States).
[3] Robertson A, Jonkman J, Masciola M, Song H, Goupee A, Coulling A and Luan C 2014 Definition of the semisubmersible floating system for phase II of OC4 (No. NREL/TP-5000-60601). National Renewable Energy Lab.(NREL), Golden, CO (United States).
[4] Jonkman J 2010 Definition of the Floating System for Phase IV of OC3 (No. NREL/TP-500-47535). National Renewable Energy Lab.(NREL), Golden, CO (United States).
[5] Roddier D, Cermelli C, Aubault A and Weinstein A 2010 WindFloat: A floating foundation for offshore wind turbines, *J. Renew. Sustain. Energy*, **2**(3), 033104.
[6] DNV GL 2019 SESAM User Manual, WADAM (Høvik, Norway).
[7] Liang G, Merz K and Jiang Z 2020 Modeling of a Shared Mooring System for a Dual-Spar Configuration *Int. Conf. on OMAE* (American Society of Mechanical Engineers) vol 84416.
[8] Li L, Gao Z., Moan T 2015 Joint Distribution of Environmental Condition at Five European Offshore Sites for Design of Combined Wind and Wave Energy Devices, *J. Offshore Mech. Arct. Eng*. **137**(3).
[9] Jonkman B J and Buhl Jr. M L 2006 Turbsim user's guide. Tech. rep., National Renewable Energy Lab.(NREL), Golden, CO (United States).
[10] IEC, 2005. International standard IEC 61400-1, Wind turbines—Part 1: Design requirements (Geneva, Switzerland).
[11] IEC, 2009. International standard IEC 61400-3, Wind turbines—Part 3: Design requirements for offshore wind turbines (Geneva, Switzerland).
[12] SINTEF Ocean 2019. SIMO 4.10.1 User Guide (Trondheim, Norway).
[13] SINTEF Ocean 2019. RIFLEX 4.16.0 User Guide (Trondheim, Norway).

Appendix A

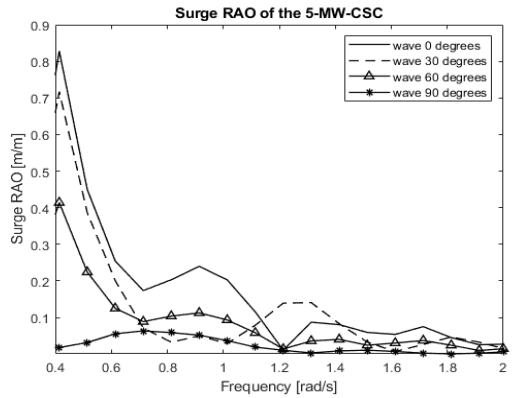

Figure 12. Surge RAO of the 5-MW-CSC

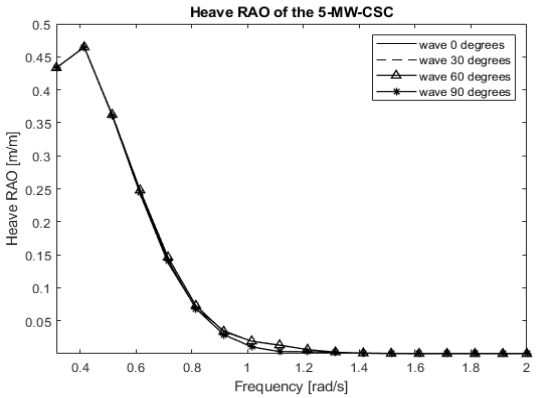

Figure 13. Heave RAO of the 5-MW-CSC

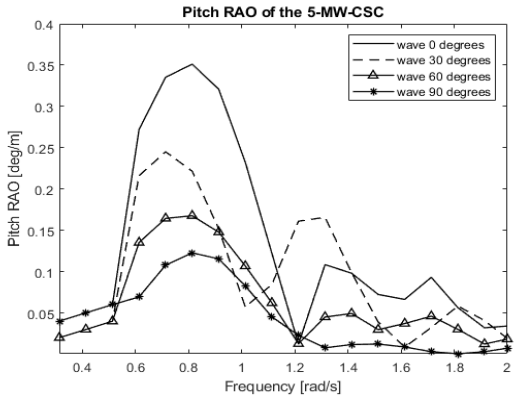

Figure 14. Pitch RAO of the 5-MW-CSC